Title
Plasma heating with a rotating relativistic electron beam. II. Magnetosonic wave emission

Journal
Physics of Fluids, 20(3)

ISSN
00319171

Authors
Molvig, Kim
Rostoker, Norman

Publication Date
1977

DOI
10.1063/1.861889

Peer reviewed

Plasma heating with a rotating relativistic electron beam. II. Magnetosonic wave emission

Kim Molvig

Physics Department, University of California, Irvine, California 92664
and Research Laboratory of Electronics, Massachusetts Institute of Technology, Cambridge, Massachusetts 02139

Norman Rostoker

Physics Department, University of California, Irvine, California 92664
(Received 29 December 1975; final manuscript received 16 November 1976)

The magnetosonic wave emission by an intense relativistic electron beam rotating within a plasma is calculated. This process follows the trapping of the beam in the plasma, and results in a transfer of approximately half the beam energy to the plasma ions. A nonlinear theory is given in accord with beam and plasma parameters of fusion interest. It is shown that dissipation balances the nonlinearity to produce a shock-type flow resembling that of the linear theory. The primary nonlinear modification is an adjustment of the wave speed to $v_s = v_A M_s$, where $v_A^2 = B_0^2/4\pi n m_i$ and $M_s = 1 + \tilde{B}/B_0$ is the mach number ($\tilde{B}$ is the wave field, B_0 is the applied field). Estimates are made of power radiated to the waves and the resultant ion energies for some typical experimental parameters.

I. INTRODUCTION

We consider the second stage of the interaction after the beam has been trapped in the plasma by the mechanism discussed in (I).[1] This process is assumed to have occurred in a reasonably coherent manner so that the beam retains its annular shape and high rotational velocity. For simplicity, the axial variations are neglected. The conditions prevailing immediately behind the beam head in the propagating beam are assumed to exist throughout the range of z at the time propagation stops. The trapping phase of the interaction is treated as a transient occurring prior to $t=0$, so that the second stage may be formulated mathematically as an initial value problem. Beam dynamics are neglected, so that the beam provides a fixed current source. In general, in this paper we do not consider instabilities except in the peripheral sense that they may cause an anomalous electron-ion collision frequency.

There are two cases to distinguish depending on whether the magnetosonic mode is or is not critically damped. In the former case, as was discussed in (I) both the Langevin and momentum conserving collision terms have the same consequences for the propagating beam. The plasma response is essentially a diffusion process and energy is transferred Ohmically to the plasma. If the collision frequency is large enough to produce the critical damping, then the formulae in (I) may be applied by simply making the change

$$-z/v_{\parallel} + t \to t.$$

Specifically, Eq. (52) of (I) the power dissipated per unit length by the angular current, becomes

$$P_d = \pi \frac{I_{b\theta}^2}{\sigma_f}\left(1 + \frac{4D_f t}{a^2}\right)^{-2}. \tag{1}$$

Dissipation occurs for a time given effectively by $\tau_d = a^2/4D_f$, and the total energy deposited in plasma is

$$U_d = \pi^2 (a^2/c^2) I_{b\theta}^2, \tag{2}$$

which is independent of the conductivity. Comparing this to the beam energy density $U_b = \pi a^2 n_b (\gamma - 1) mc^2$ (using $I_{b\theta} \cong a n_c e c$), we find

$$U_d / U_b = \frac{\nu}{\gamma - 1}, \tag{3}$$

where $\nu \equiv \pi a^2 (e^2/mc^2)\, n_b$ is the number of beam electrons per classical electron radius. Thus, for either a high energy ($\gamma \gg 1$) and large ν/γ beam, or a low energy ($\gamma \ll 1 + 1/\nu$) beam, all beam energy goes into the plasma in a fraction of the diffusion time, τ_d.

To determine how the energy distributes among the various ion, electron, and wave components, one needs a detailed understanding of the dissipative process which our phenomenological treatment does not allow. Indeed, to maintain the collision frequency at the magnitude needed for critical damping of the magnetosonic wave requires a strongly turbulent state. Since there is no satisfactory theory of this, we have used estimates of the collision frequency based on experiments and weak turbulence theory. This will give reasonable results for dissipated power when the phenomenological constants are accurate, but cannot give the distribution of energy within the plasma.

The second case, when the magnetosonic mode is not critically damped, is the primary subject of this paper. This can occur even when the mode is critically damped initially since plasma electrons are substantially heated during trapping. Also, turbulent enhancement of the collision frequency may subside in the approximately 100 nsec it takes the beam to stop. In any event, if excited, the magnetosonic disturbance should be large, and one does not expect a linear treatment to be valid. It turns out, however, that for the configuration and parameters considered here, the linear, collisionless, nondispersive version of the theory actually gives quite good results. This happens because the beam creates a shock type disturbance. Nonlinear wave front steepen-

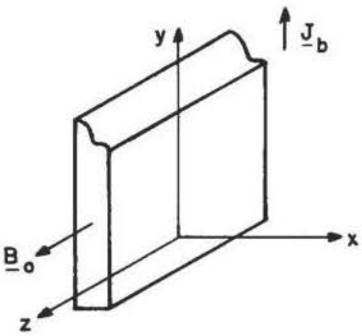

FIG. 1. Slab geometry for magnetosonic wave emission.

ing is balanced by dissipation to produce a flow resembling that calculated from linear theory. The only significant modification to the linear theory is an increase in the propagation speed $v_s \to M_s v_A$, where $M_s \equiv 1 + \Delta B / B_0$ is the Alfvén mach number and $v_A = B_0^2/(4\pi n m_i)^{1/2}$ is the Alfvén speed. We show this with a weakly nonlinear calculation in Sec III. The linear results which thus have a somewhat undeserved validity, are given in Sec. II. The overall implications as well as some numerical estimates for experiments are considered in Sec. IV.

II. LINEAR MAGNETOSONIC WAVE EMISSION

We consider the geometry of Fig. 1, which depicts a slab beam. This approximates the thin annular beam but ignores cylindrical effects. The convergence of the inward propagating wave and its reflection from the cylinder axis is thus neglected. Beam current is flowing in the y direction and the wave will propagate in the x direction. The system we have in mind is the same as in (I) but not propagating, as summarized in Table I.

After Fourier–Laplace transforming Maxwell's equations, with the plasma dielectric function inserted we have

$$\mathbf{k}\times(\mathbf{k}\times\mathbf{E}) + \frac{\omega^2}{c^2}\,\boldsymbol{\epsilon}\cdot\mathbf{E} = \frac{i\omega}{c^2}\,\mathbf{E}\Big|_{t=0} + \frac{1}{c^2}\,\frac{\partial}{\partial t}\,\mathbf{E}\Big|_{t=0} - \frac{4\pi i\omega}{c^2}\,\mathbf{J}_b - \frac{4\pi}{c^2}\,\mathbf{J}_b\Big|_{t=0} - \frac{4\pi}{c^2}\,\mathbf{J}_p\Big|_{t=0}, \tag{4}$$

where the initial value terms have been written in terms of the electric field and plasma current. Starting from the neutralized initial condition, $\mathbf{J}_p = -\mathbf{J}_b$, $(\partial/\partial t)\mathbf{E}|_{t=0} = 0$, and neglecting axial variations for the nonpropagating beam, (4) may be written

$$\mathbf{D}\cdot\mathbf{E} = (c^2/\omega^2)\,\mathbf{S}, \tag{5}$$

where

$$\mathbf{S} = \frac{i\omega}{c^2}\,\mathbf{E}_k^0 - \frac{4\pi i\omega}{c^2}\,\mathbf{J}^b_{k,\omega}, \tag{6}$$

$$\mathbf{D} = \begin{bmatrix} \epsilon_\perp & i\epsilon_H \\ -i\epsilon_H & \epsilon_\perp - n^2 \end{bmatrix}, \tag{7}$$

and $n = kc/\omega$ is the index of refraction. The dielectric coefficients are those obtained from the cold, collisionless two-fluid equations and are given by

$$\epsilon_\perp = 1 + \frac{\omega_{pe}^2}{\omega_{ce}^2 - \omega^2} + \frac{\omega_{pi}^2}{\omega_{ci}^2 - \omega^2}, \tag{8}$$

$$\epsilon_H = \frac{\omega_{ce}}{\omega}\,\frac{\omega_{pe}^2}{\omega_{ce}^2 - \omega^2} - \frac{\omega_{ci}}{\omega}\,\frac{\omega_{pi}^2}{\omega_{ci}^2 - \omega^2}. \tag{9}$$

The dispersion tensor $\mathbf{D}$ becomes more symmetric in a coordinate system where the $\mathbf{k}$ vector lies at 45° to the x axis. This transformation is accomplished with the rotation matrix

$$\mathbf{R} = \frac{1}{\sqrt{2}}\begin{bmatrix} 1 & -1 \\ 1 & 1 \end{bmatrix}, \tag{10}$$

$$\mathbf{D}' = \mathbf{R}^{-1}\cdot\mathbf{D}\cdot\mathbf{R} = \begin{bmatrix} D_\perp & D_H \\ D_H^* & D_\perp \end{bmatrix}, \tag{11}$$

where

$$D_\perp = \epsilon_\perp - n^2/2; \quad D_H = i\epsilon_H - n^2/2. \tag{12}$$

Eigenvalues of $\mathbf{D}'$ are

$$\lambda = D_\perp \mp |D_H|. \tag{13}$$

Defining the phase of D_H by $D_H = |D_H|\,e^{i\phi}$, the eigenvector matrix which diagonalizes $\mathbf{D}'$ is

$$\mathbf{T} = \frac{1}{\sqrt{2}}\begin{bmatrix} e^{i\phi/2} & e^{i\phi/2} \\ -e^{-i\phi/2} & e^{-i\phi/2} \end{bmatrix}. \tag{14}$$

Thus, the composite transformation to diagonalize the initial dispersion tensor, Eq. (7), becomes

$$\mathbf{O} = \mathbf{R}\cdot\mathbf{T} = \begin{bmatrix} \cos(\phi/2) & i\sin(\phi/2) \\ i\sin(\phi/2) & \cos(\phi/2) \end{bmatrix}. \tag{15}$$

Applying this to Eq. (5) results in the decoupled mode equations

$$[D_\perp - |D_H|]\,E_1' = (c^2/\omega^2)\,S_1', \tag{16}$$

$$[D_\perp + |D_H|]\,E_2' = (c^2/\omega^2)\,S_2', \tag{17}$$

where the primed source and field components are related to the x, y components by

$$E' = \mathbf{O}^\dagger\cdot\mathbf{E}; \quad \mathbf{S}' = \mathbf{O}^\dagger\cdot\mathbf{S}, \tag{18}$$

TABLE I. Numerical estimates for a plasma heating experiment. The last two rows give the collision frequencies and stopping length expected during the trapping phase, using Eq. (74) of (I), with $v_\parallel = 0.1c$ and $f = 1$.

	$\gamma = 3$, $B_0 = 1$ kG	$\gamma = 30$, $B_0 = 10$ kG
r_0 cm	5.	5.
a cm	1.	1.
n_b cm^{-3}	$1.\times10^{11}$	$2.\times10^{12}$
n_p cm^{-3}	$1.\times10^{13}$	$1.\times10^{14}$
E_x kV/cm	1.5	30.
B k-G	0.3	6.
v_s cm/sec	4.5×10^{7}	$14.\times10^{7}$
E_i eV	225.	9000.
τ nsec	250.	60.
ν_e sec^{-1}	10^{8}	10^{9}
l_s cm	45.	22.5

where $\mathbf{O}^\dagger$ denotes the Hermitian conjugate matrix.

Now, in the normal mode equations (16), (17), $D_\perp$ is negative for real ω. This means that in carrying out the ω inversion integral for E_1' no poles will be encountered on the real ω axis. Accordingly, E_1' represents an evanescent response and is not of interest. E_2' is the actual normal mode amplitude. Its polarization is given by the second column of the $\mathbf{O}$ matrix

$$\frac{E_x}{E_y} = i \tan \frac{\phi}{2} = -i \frac{\epsilon_H}{\epsilon_\perp}, \tag{19}$$

where the last equality is obtained by using the dispersion relation $D_\perp^2 - |D_H|^2 = 0$. This is the same polarization as in the homogeneous solution $\mathbf{D} \cdot \mathbf{E} = 0$ [see Eq. (7)].

We now specialize to the case of a magnetosonic mode in a dense, $\omega_{pe}^2/\omega_{ce}^2 \gg 1$, plasma. The frequency regime is

$$\omega_{ci}^2 \ll \omega^2 \ll \omega_{ci}\omega_{ce}, \tag{20}$$

as will be self-consistently verified shortly. In this limit, the dielectric coefficients simplify considerably

$$\epsilon_\perp \cong -(\omega_{pe}^2/\omega^2)(\omega_{ci}/\omega_{ce}), \tag{21}$$

$$\epsilon_H \cong (\omega_{pe}^2/\omega^2)(\omega/\omega_{ce}), \tag{22}$$

and the polarization becomes $E_x/E_y = i(\omega/\omega_{ci})$. The term "magnetosonic" is usually applied to the limit $\omega \ll \omega_{ci}$, in which case the electric field polarization is transverse. For the case considered here, we retain the terminology, although the mode is somewhat different and is polarized primarily in the longitudinal direction.

The dispersion relation, which is $D_\perp^2 - |D_H|^2 = 0$, or $\epsilon_\perp^2 - \epsilon_\perp n^2 - \epsilon_H^2 = 0$, is now $\omega^2 = k^2 v_A^2$. Thus, the condition [Eq. (20)] becomes

$$\omega_i/\omega_{ce} \ll k^2c^2/\omega_{pe}^2 \ll 1 ,$$

and for a 1 cm thick beam and 10^{14} cm^{-3} plasma the inequlity is justified to the extent that $1/2000 \ll 1/10 \ll 1$.

Calculating the transverse field component, we find

$$E_y = \frac{c^2}{\epsilon_H} \frac{1}{\omega^2 - k^2 v_A^2} S_2', \tag{23}$$

and the mode source is

$$S_2' = -iS_x + (\epsilon_H/n^2) S_y. \tag{24}$$

The longitudinal source, S_x, arises from the Hall field of the angular return current and is an initial value term. S_y has contributions from the beam current and the initial electric field, although the latter may be neglected. Taking the beam current to be constant in time, with the same x dependence as the initial E_x (this follows from the angular return current calculation when the decay is neglected), and denoting $R = J_b/E_x$, we have

$$S_2' = \frac{1}{c^2}\left(\omega - 4\pi \frac{\epsilon_H}{n^2} R\right)\epsilon(k), \tag{25}$$

where $\epsilon(k)$ is the Fourier transform of source. The first term is due to the initial electric field and the second to the beam current.

After carrying out the ω inversion, the transverse field in Eq. (23) is expressed as

$$E_y(x,t) = \tfrac{1}{2} i2\pi \int dk\, \epsilon(k)\, kv_A\left(\frac{\omega_{ce}}{\omega_{pe}^2} - \frac{v_A^2}{c^2}\frac{4\pi R}{k^2 v_A^2}\right) \times\{\exp[ik(x+v_At)] - \exp[ik(x-v_At)]\} \tag{26}$$

where $v_A \equiv (B^2/4\pi n M_i)^{1/2}$ is the Alfvén speed. The response to the initial disturbance can be expressed as a derivative of the forward and backward propagated pulses, the response to the beam current as an integral. This makes the resulting distrubances occur in somewhat different places, although for a localized sheet source the differences are minor. Comparing magnitudes, and using $R = \omega_{pe}^2/4\pi\omega_{ce}$, the beam current term is bigger than the initial E_x term by the factor

$$\omega_{pi}^2/\omega^2 \gg 1,$$

so that the initial value term may be neglected.

This finally gives

$$E_y(x,t) = \frac{v_A}{c}\frac{4\pi R}{2c}\int_{x-v_At}^{x+v_At} d\xi\, E(\xi), \tag{27}$$

with $RE(\xi)$ the beam current distribution.

The basic features can be seen from the response to a sheet beam current distribution

$$RE(x) = I_0\delta(x),$$

where I_0 is current per unit length of beam. For the resulting transverse field, we find

$$E_y = \frac{v_A}{c}\frac{4\pi I_0}{c}\frac{1}{2}[H(x+v_At) - H(x-v_At)], \tag{28}$$

where H is the Heaviside unit step function. The remaining quantities are related to E_y by constant multiplicative factors and differentiation. These relations are given in the following section, where the method in the nonlinear calculation requires the full linear eigenvector. Equation (47) lists the eigenvector for forward propagating waves. The backward wave eigenvector is obtained from Eq. (47) by changing the sign of v_A. Using these we obtain

$$E_x(x,t) = V_0 \tfrac{1}{2}[(x+v_At) + \delta(x-v_At)], \tag{29}$$

$$B_z(x,t) = (2\pi I_0/c)[-H(x+v_At) + 2H(x) - H(x-v_At)], \tag{30}$$

$$v_{ix}(x,t) = v_A(B/B_0)[H(x+v_At) - H(x-v_At)], \tag{31}$$

$$J_y^p(x,t) = I_0\tfrac{1}{2}[\delta(x+v_At) + \delta(x-v_At)], \tag{32}$$

where $B = 2\pi I_0/c$ is the wave magnetic field amplitude. V_0 is the voltage drop across the beam in the angular return current interaction, i.e., $V_0 = E_r d$, and is related to the beam current by $V_0/d = \sigma_H I_0$.

Figures 2(a)–(c) summarize Eqs. (28)–(32). Under conditions where the magnetosonic mode can propagate, it carries away the neutralizing current. Accordingly, a diamagnetic B field appears inside the beam (negative x), and a paramagnetic B outside. As the inward and outward propagating pulses pass through the plasma, a flow of ions in the radial (positive x) direction is set up. Almost all of the particle energy is in this flow.

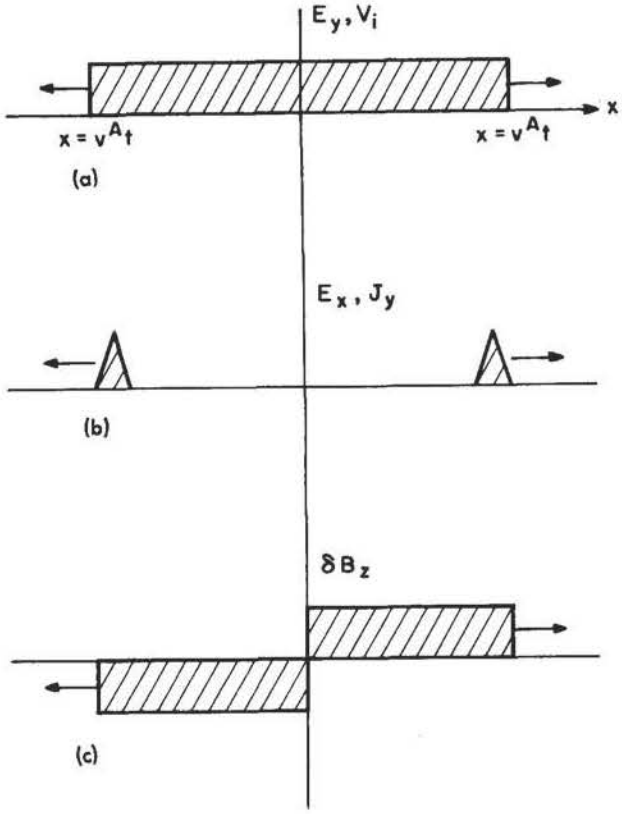

FIG. 2. Field components in magnetosonic pulse.

III. NONLINEAR EVOLUTION OF MAGNETOSONIC WAVES

The object of this section is to obtain an evolution equation for magnetosonic disturbances, including finite amplitude effects. In the absence of dissipation, it is well known[2] that the mode, in the cold fluid description, sustains stationary solutions of the soliton not the shock type. With dissipation, stationary shock solutions can be obtained. In both cases the disturbance is made stationary by a balance between dispersion and nonlinear effects.

Thus, in a perturbation expansion these competing effects must be made to enter at the same order. Otherwise, the solution obtained is not uniform and the expansion will break down in a finite time. The method then, is to take one propagation direction, and treat the $\omega = v_s k$ approximation to the wave as the first order solution. All corrections to this approximation (nonlinear, dispersive and dissipation effects) are moved to the next order. In the wave frame, the first-order equations make no restrictions at all on the functional form of the mode amplitude; it can be an arbitrary function of $x - v_S t$. (Variations must be fairly slow to justify the expansion.) What the first order equations do determine is the mode structure or eigenvector: $\mathbf{e} = (\mathbf{v}_i, \mathbf{v}_e, \mathbf{E}, \mathbf{B})\,\psi(x, t)$, physical variables in terms of a scalar mode amplitude. One can then proceed to the next order, and by a number of techniques for finding uniform expansions,[3] determine the (slow) evolution of the amplitude ψ. We will use the method of multiple time scales.[4] The expansion parameter will not be made explicit, since it is our purpose to obtain all terms that may balance the nonlinearity in the next order. Roughly, it would be related to the dimensionless mode amplitude, and parameters describing the degree of dispersion and dissipation. These emerge naturally in the resulting evolution equation.

The configuration is the same as in the previous calculation (depicted in Fig. 1). We use the cold two-fluid equations with collision terms $-m_e\nu_{ei}(\mathbf{v}_e - \mathbf{v}_i)$ for electrons, $-m_e\nu_{ei}(\mathbf{v}_i - \mathbf{v}_e)$ for ions.

Wave frame variables are

$$x = x - v_S t,\qquad t = t, \tag{33}$$

so that derivatives transform according to

$$\frac{\partial}{\partial t} \to \frac{\partial}{\partial t} - v_S\frac{\partial}{\partial x},\qquad \frac{\partial}{\partial x} \to \frac{\partial}{\partial x}. \tag{34}$$

The time derivative in the wave frame is then expanded with multiple scales

$$\frac{\partial}{\partial t} = \frac{\partial}{\partial \tau_0} + \frac{\partial}{\partial \tau_1} + \ldots \tag{35}$$

and $\partial/\partial\tau_1$ is first order in the expansion parameter.

From geometrical symmetries, the nonzero field components are

$$\mathbf{E} = (E_x, E_y, 0),\qquad \mathbf{B} = (0, 0, B),\qquad \mathbf{v} = (v_x, v_y, 0), \tag{36}$$

so that the relevant fluid Maxwell equations may be written out as

$$\frac{\partial}{\partial\tau_0} v_{ex} - v_S\frac{\partial}{\partial x} v_{ex} + \frac{e}{m_e}E_x + v_{ey}\omega_{ce} = -\frac{\partial}{\partial\tau_1}v_{ex} - \nu_{ei}(v_{ex} - v_{ix}) - \frac{e}{m_e c}v_{ey}B - v_{ex}\frac{\partial}{\partial x}v_{ex} \tag{37}$$

$$\frac{\partial}{\partial\tau_0} v_{ey} - v_S\frac{\partial}{\partial x} v_{ey} + \frac{e}{m_e}E_y - v_{ex}\omega_{ce} = -\frac{\partial}{\partial\tau_1}v_{ey} - \nu_{ei}(v_{ey} - v_{iy}) + \frac{e}{m_e c}v_{ex}B - v_{ex}\frac{\partial}{\partial x}v_{ey}, \tag{38}$$

$$\frac{\partial}{\partial\tau_0} v_{ix} - v_S\frac{\partial}{\partial x} v_{ix} - \frac{e}{m_i}E_x - v_{iy}\omega_{ci} = -\frac{\partial}{\partial\tau_1}v_{ix} - \nu_{ei}\frac{m_e}{m_i}(v_{ix} - v_{ex}) + \frac{e}{m_i c}v_{iy}B - v_{ix}\frac{\partial}{\partial x}v_{ix}, \tag{39}$$

$$\frac{\partial}{\partial\tau_0} v_{iy} - v_s\frac{\partial}{\partial x} v_{iy} - \frac{e}{m_i}E_y + v_{ix}\omega_{ci} = -\frac{\partial}{\partial\tau_1}v_{iy} - \nu_{ei}\frac{m_e}{m_i}(v_{iy} - v_{ey}) - \frac{e}{m_i c}v_{ix}B - v_{ix}\frac{\partial}{\partial x}v_{iy}, \tag{40}$$

$$\frac{\partial}{\partial\tau_0} n_e - v_s\frac{\partial}{\partial x} n_e + n_0\frac{\partial}{\partial x} v_{ex} = -\frac{\partial}{\partial\tau_1} n_e - \frac{\partial}{\partial x} n_e v_{ex}, \tag{41}$$

$$\frac{\partial}{\partial \tau_0} n_i - v_s \frac{\partial}{\partial x} n_i + n_0 \frac{\partial}{\partial x} v_{ix} = -\frac{\partial}{\partial \tau_1} n_i - \frac{\partial}{\partial x} n_i v_{ix} \qquad (42)$$

$$+\frac{1}{c}\frac{\partial}{\partial \tau_0} B + \frac{\partial}{\partial x} E_y - \frac{v_s}{c}\frac{\partial}{\partial x} B = -\frac{1}{c}\frac{\partial}{\partial \tau_1} B, \qquad (43)$$

$$-\frac{1}{c}\frac{\partial}{\partial \tau_0} E_y - \frac{\partial}{\partial x} B - \frac{4\pi e n_0}{c}(v_{iy} - v_{ey}) + \frac{v_s}{c}\frac{\partial}{\partial x} E_y = \frac{1}{c}\frac{\partial}{\partial \tau_1} E_y + \frac{4\pi e}{c}(n_i v_{iy} - n_e v_{ey}), \qquad (44)$$

$$-\frac{\partial}{\partial \tau_0} E_x - \frac{4\pi e n_0}{c}(v_{ix} - v_{ex}) + \frac{v_s}{c}\frac{\partial}{\partial x} E_x = +\frac{1}{c}\frac{\partial}{\partial \tau_1} E_x + \frac{4\pi e}{c}(n_i v_{ix} - n_e v_{ex}). \qquad (45)$$

The definitions $\omega_{ce} \equiv |eB^{(0)}/m_e c|$, $\omega_{ci} \equiv |eB^{(0)}/m_i c|$, of cyclotron frequencies in the zero order magnetic field, have been used. $B^{(0)}$ is not equal to the applied field but will be determined at the end of the calculation. Corrections to gyration frequencies due to the wave field, B, appear on the right-hand side of the equations. This nonlinearity will contribute terms identical to those resulting from the convective derivative. Equations (37)–(45) constitute a complete set. Poison's equation is redundant in this geometry, since it may be deduced from Eqs. (41), (42), and (45).

The first-order solution is given by the left-hand side of Eqs. (37)–(45), which still contain some unwanted dispersion terms. We are interested in a solution which, linearly, is stationary. Thus, the fast time derivative of first-order terms is assumed to be zero. Solving the left-hand side by essentially algebraic manipulations, gives

$$-\frac{v_s c^2}{4\pi n_0 e}\frac{\partial^3}{\partial x^3} E_y + \left(v_s \frac{e}{m_e} - \omega_{ce}\omega_{ci}\frac{c^2}{v_s 4\pi n_0 e}\right)\frac{\partial}{\partial x} E_y = 0. \qquad (46)$$

The solution also yields the eigenvector

$$\begin{aligned}
B &= (c/v_s) E_y,\\
v_{ey} &= \frac{c}{v_s}\frac{c}{4\pi n_0 e}\frac{\partial}{\partial x} E_y,\\
v_{ex} &= \frac{c^2}{v_s^2}\frac{\omega_{ci}}{4\pi n_0 e} E_y,\\
E_x &= -\frac{c}{v_s}\frac{B^{(0)}}{4\pi n_0 e}\frac{\partial}{\partial x} E_y,\\
v_{iy} &= -(m_e/m_i) v_{ey},\\
v_{ix} &= v_{ex},\\
n_e &= (n_0/v_s) v_{ex},\\
n_i &= (n_0/v_s) v_{ix}.
\end{aligned} \qquad (47)$$

Numerical factors of order m_e/m_i, v_s/c have been neglected.

Now, if the dispersion term in Eq. (46) is ignored, and the velocity v_s is chosen to satisfy $v_s^2/c^2 = \omega_{ce}\omega_{ci}/\omega^2$, then the first-order solution is simply the eigenvector, Eq. (47). The x dependence is arbitrary and quantities do not vary on the fast time scale.

To remove dispersion from the first order equations, the terms giving rise to it must be identified. This can be done by inserting the eigenvector Eq. (47) in the left-hand side of Eqs. (37)–(45). All equations collapse to zero except Eqs. (38) and (40) in which inertial terms $-v_s(\partial/\partial x) v_{ey}$ and $-v_s(\partial/\partial x) v_{iy}$ fail to cancel. These thus cause the dispersion, are second order quantities, and in future discussions will be considered to be on the right-hand side.

The sequence of operations on Eqs. (37)–(45) which gives Eq. (46) is

$$\omega_{ci}\left[-\frac{c}{v_A}(43) + (44)\right] - \frac{4\pi e n_0}{c}\left[-\frac{v_s}{\omega_{ce}}\frac{m_e}{m_i}\frac{\partial}{\partial x}(38) + \frac{v_s}{\omega_{ci}}\frac{\partial}{\partial x}(40) + \frac{m_e}{m_i}(37) + (39)\right]. \qquad (48)$$

Note that the continuity equations (41), (42), and also (45) do not enter. Equations (41) and (42) are solved independently by $n = (n_0/v_s) v_x$, while Eq. (45) is higher order.

Now, consider the next order in perturbation theory. It may be written, formally, as

$$\frac{\partial}{\partial \tau_0}\mathbf{e}^{(2)} + \mathbf{L}\cdot\mathbf{e}^{(2)} = \mathbf{e}_{ms}\frac{\partial}{\partial \tau_1}\psi^{(1)} + \mathbf{N}(\mathbf{e}_{ms}\psi^{(1)}), \qquad (49)$$

where $\mathbf{e}^{(2)}$ is the second-order (vector) solution, $\mathbf{L}$ is a linear differential operator [from the left-hand side of Eqs. (37)–(45) and without dispersion terms], $\mathbf{e}_{ms}$ is the magnetosonic eigenvector Eq. (47), $\psi^{(1)}$ is the first-order amplitude, and $\mathbf{N}$ is the nonlinear operator given by the right-hand side of Eqs. (37)–(45). In principal, if one has all the eigenvectors of $\mathbf{L}$ [Eq. (47) is one of them], Eq. (49) can be diagonalized and the components of $\mathbf{e}^{(2)}$ calculated independently. These components correspond to evanscent "modes" in addition to all the normal modes. The evanscent components may be neglected but generally other phenomena, such as nonlinear decays, will occur. Since the magnetosonic wave is the lowest frequency mode (for perpendicular propagation), it does not drive decay instabilities. We, therefore, need only $\mathbf{e}_{ms}$ dotted into Eq. (49) which describes the interaction of the magnetosonic mode with itself.

The operations of Eq. (48) are equivalent to the $\mathbf{e}_{ms}$ dot product and when carried out on Eq. (49) reduce $\mathbf{L}\mathbf{e}^{(2)}$ to zero, that is, the eigenvalue corresponding to $\mathbf{e}_{ms}$ is zero. This second-order equation is

$$\frac{\partial}{\partial \tau_0}\psi^{(2)} = -2\frac{L}{v_s T}\frac{\partial}{\partial \tau_1} B - 5B\frac{\partial}{\partial x} B + \frac{c^2}{\omega_{pe}^2 L^2}\left(\frac{\nu_{ei} L}{v_s} + \frac{\partial}{\partial x} B\right)\frac{\partial^2}{\partial x^2} B - \frac{c^2}{\omega_{pe}^2 L^2}(1 - B)\frac{\partial^3}{\partial x^3} \times B + \frac{c^2}{\omega_{pe}^2 L^2}\frac{L}{v_s T}\frac{\partial^3}{\partial \tau_1 \partial x^2} B, \qquad (50)$$

and is given in dimensionless form. Spatial and temporal scales are denoted by L and T. The first-order amplitude is expressed in terms of B, the wave magnetic field, scaled to the zero-order field.

The requirement that the expansion be uniform or without time secularities leads immediately to $\partial\psi^{(2)}/\partial\tau_0 = 0$, and the desired evolution equation is obtained. If we further discard terms of an obviously higher order it may be written

$$0 = 2\frac{L}{v_s T}\frac{\partial}{\partial\tau_1}B + 5B\frac{\partial}{\partial x}B - \frac{c^2}{\omega_{pe}^2 L^2}\frac{\nu_{ei}L}{v_s}\frac{\partial^2}{\partial x^2}B + \frac{c^2}{\omega_{pe}^2 L^2}\frac{\partial^3}{\partial x^3}B. \tag{51}$$

The first three terms give the Burgers equation, the first, second and last, the Korteweg–deVries equation. For the case we have been considering ($L \sim 1$, $\nu \sim 10^9$, $n_p \sim 10^{14}$, $B^{(0)} \sim 1\,G$), $c^2/\omega_{pe}^2 L^2 \sim 1/400$, $\nu_{ei}L/v_s \sim 100$, so that the last term has a very small effect. Neglecting, this, and deleting the slow time notation finally results in

$$0 = 2\frac{L}{v_s T}\frac{\partial}{\partial t}B + 5B\frac{\partial}{\partial x}B - \frac{c^2}{\omega_{pe}^2 L^2}\frac{\nu_{ei}L}{v_s}\frac{\partial^2}{\partial x^2}B. \tag{52}$$

Note that the dissipation, which appeared as a friction proportional to the velocity in the fluid equations, contributes as a diffusion term in the evolution equation.

The stationary solution to Eq. (52) may be obtained by two elementary integrations

$$B = \Delta B \tanh\left[-\tfrac{1}{2}(\Delta B/\mu)(x - x_0)\right], \tag{53}$$

where $\mu = \frac{1}{5}(c^2/\omega_{pe}^2 L^2)(\nu_{ei}L/v_s)$, and ΔB is the amplitude. These are shock type solutions, with the shock width given by $(\mu/\Delta B)L$. In the laboratory variables, $x \to x - v_s t$, the disturbance propagates.

The magnetic field in Eq. (53) goes from ΔB at $x = -\infty$ to $-\Delta B$ at $x = \infty$, whereas in the usual problem, one has the perturbation zero at $x = \infty$. Thus, in order to satisfy the boundary conditions the zero order field, $B^{(0)}$, must be chosen as $B^{(0)} = B_0 + \Delta B$ where B_0 is now the applied field. This *a posteriori* selection of $B^{(0)}$ introduces a nonlinear correction to the wave speed according to

$$v_s = \frac{B^{(0)}}{(4\pi n m_i)^{1/2}} = v_A\left(1 + \frac{\Delta B}{B_0}\right) = M_s v_A \tag{54}$$

where, in (54), $v_A^2 = B_0^2/4\pi n m_i$ is the Alfvén speed in the applied field, and the last equality defines the magnetosonic Mach number.

When the initial perturbation has a step of width $l \neq (\mu/\Delta B)L$, Eq. (52) will give the evolution to the final state. For $l < (\mu/\Delta B)L$, the behavior will initially be diffusion. When $l > (\mu/\Delta B)L$, the initial motion will be a steepening of the wave front.

Although this is an initial value analysis, it may be applied to the driven response problem of the rotating beam in a fairly straightforward way. Consider the diamagnetic and paramagnetic responses separately. Each, once initiated, develops in exactly the same way as an initial step function propagating wave. Making use of this equivalence we take as initial conditions the results of the linear theory a short time after the beam pulse turns on. Both para-and diamagnetic parts are extended to infinity in the direction opposite to their propagation. This is a calculational artifice and the solution in these regions is neglected. A small error may result from the initial nonlinear interaction of the two waves.

Thus, the initial distrubance has a "shock" width equal to the beam thickness, typically 1 cm. This is to be compared with the stationary shock width (in real units)

$$l_{sH} = \frac{1}{5}\frac{c^2}{\omega_{pe}^2}\frac{\nu_{ei}}{v_A}\frac{B_0}{\Delta B}. \tag{55}$$

For $\nu_{ei} \sim 10^9$, $n_p \sim 10^{14}$, $B_0 \sim 1\,\text{KG}$, $\Delta B/B_0 = 0.3$ this gives $l_{sH} = 0.1$ cm. In these late stages of the interaction, the estimate of an enhanced ν_{ei} may be too high. At $\nu_{ei} \sim 10^8$, beam and stationary shock widths are equal.

We conclude that dissipation dominates dispersive effects and combines with the nonlinearity to make a steady flow resembling the linear, nondispersive result.

Modifications to the linear theory are increased propagation speed $v_s = M_s v_A$, and a slightly modified pulse shape, Eq. (53).

IV. NUMERICAL ESTIMATES FOR EXPERIMENTS

Consider first the case when the magnetosonic mode is critically damped. Heating is then by the same process as during trapping, namely Ohmic. The parameters of Table I will be used for the estimates. At this collision frequency $\nu_{ei} \sim 10^9$, the magnetosonic mode is, marginally, critically damped [see (I)]. It should be noted that this magnitude collision frequency corresponds to an extremely high level of turbulence. If electron temperature after trapping is $\gtrsim 100$ eV, the enhancement factor of ν_{ei} over classical is $\gtrsim 10^4$. The formulae from Sec. I may be modified to apply to an annular beam. Putting $\gamma = 2$ and taking beam length to be 1 *m*

$$I_{b\theta} = aenc = 1.44 \times 10^{12}\ \text{SA/cm}$$
$$P_D = \pi I_{b\theta}^2/\sigma_{eff} = 2.1 \times 10^{-2}\ \text{J/cm} - \text{nsec},$$
$$\tau_D = \pi r_0^2 \sigma_{eff}/c^2 = 2.7\,\mu\text{sec},$$
$$U_D = 100 P_D \tau_D = 5.68\ \text{J}. \tag{56}$$

From $\nu = \pi a r_0 (e^2/mc^2) n_b$ and $U_b = \pi a r_0 n_b (\gamma - 1) mc^2$, the relation $U_D = [\nu/(\gamma - 1)]\, U_b$ can be verified. Dissipated energy represents a fraction, $\nu = 0.44$, of the beam energy. Similar estimates for the energy dissipated during trapping show it to be about 0.1 of this (assuming approximately 100 nsec for trapping time and pulse length). Parameters used apply to a quite tenuous beam, or a dense one trapped inefficiently. A 100 kA, 50 nsec beam pulse injected into the same volume would result in a density, $n_b > 10^{13}$ cm^{-3}.

For the noncritically damped case we may use the results of linear theory after making the replacement $v_A \to v_S = M_S v_A$. None of the quantities to be calculated here depend on the shock width. The change in field energy after passage of the shock is

$$\Delta U_b = (BB_0/4\pi) + (B^2/8\pi).$$

When paramagnetic and diamagnetic parts are taken together, the cross terms in the field energy will cancel (neglecting cylindrical effects), so we need to consider the wave field energy only. This is equal to the ion flow energy and other contributions are negligible

$$U_b = U_i = \tfrac{1}{2}(\pi I_0^2/c^2) = \tfrac{1}{2}\pi a^2 e^2 n_b^2, \tag{57}$$

where I_0 is the beam current per unit length and a is the beam thickness. Power flow per unit area into the waves including ingoing and outgoing parts is thus

$$P = 4U_b v_s = 2\pi a^2 e^2 n_b^2 v_s. \tag{58}$$

Beam energy is completely dissipated in a time

$$\tau = (r_0/v_s)[(\gamma - 1)/\nu] \tag{59}$$

where the beam ν is $2\pi r_0 a(e^2/mc^2) n_b$ (a is beam thickness, and r_0 is beam radius). It follows from Eq. (57) that ion energy scales like n_b^2/n_p, and is given by

$$E_i = \nu(n_b/n_p)(a/4r_0)\, mc^2. \tag{60}$$

Table I summarizes the results for two sets of experimental parameters. Both cases represent weakly nonlinear disturbances. The expansion parameter, approximately $B/B^{(0)} = B/B_0M_s$, is about 0.2 in the first column and 0.4 in the second. The longitudinal electric field across the shock is not large enough to reflect the ions (for the paramagnetic pulse), so that the most obvious failure of a weakly nonlinear theory can be discounted. Difficulties in the estimates are high shock speed and short beam lifetimes, especially for the case in column two. Beam current was assumed to turn on instantly and remain constant, which is a good model for trapping time short compared with both a/v_s and τ. This is clearly not the case in column two, and those numbers must therefore be considered as quite speculative. The primary error involves using the stationary nonlinear solution, since the linear problem is complex and not close to the stationary solution. The mode is still weakly nonlinear so that (51), or the equivalent with the source term, would be valid, but the detailed temporal evolution has to be considered. Quantities such as wave field and ion energy which depend only on disturbance magnitude and linear eigenvector may be considered reliable.

We have focused on the problem of coupling beam energy into plasma ions. In so doing a number of phenomena have been greatly simplified or ignored entirely. Some of these and possible consequences are as follows.

Finite plasma temperature can have two effects. The first comparatively minor one is to modify magnetosonic propagation speed. For expected initial plasma temperature this would be a negligible effect. Second, pressure gradients can drive the mode. This can become significant when plasma electrons are highly heated during beam trapping. Modifications of the previous model are possible (hot fluid) to permit calculating the effect in the same manner.

Dissipation within the shock is a higher-order process, which in this expansion determined the shock structure but did not affect energy balance. Eventually, the wave decays due to this dissipation. A related question is thermalization of the ion flow. These mechanisms are not expected to greatly affect the coupling of beam energy to the mode.

Finally, there are finite boundary effects. The waves reflect from the plasma boundary and cylinder axis to return and interact with each other and again with the beam. Moreover, there is geometric focusing. This can be a very significant phenomena for the inward propagating wave which converges in approaching the axis. Thus for our parameters, a 10 cm diameter cylindrical shock approximately 1 cm in width would focus to approximately 2 cm diam, increasing the Mach number to about 3, and becoming a very strong shock.

ACKNOWLEDGMENTS

We would like to thank G. Benford, A. Fisher, C. W. Roberson, and T. Tajima for their discussion of this problem.

The work was supported in part by Energy Research and Development Administration, contracts AT(04-3) 34 PA207 (University of California, Irvine) and E(11-1) -3070 (Massachusetts Institute of Technology).

[1]K. Molvig and N. Rostoker, Phys. Fluids 20, 494 (1977).

[2]D. A. Tidman and N. A. Krall, *Shock Waves in Collisionless Plasmas* (Wiley, New York, 1971), Chap. 3.

[3]A. H. Nayfeh, *Perturbation Methods* (Wiley, New York, 1973).

[4]G. Sandri, Nuovo Cimento 26, 67 (1965).